Supplementary Information to *Closing the Plio-Pleistocene ^{13}C cycle in the 405-kyr periodicity by isotopic signatures of geological sources*

Peter Köhler[1]

[1]Alfred-Wegener-Institut Helmholtz-Zentrum für Polar- und Meeresforschung, P.O. Box 12 01 61, 27515 Bremerhaven, Germany

Correspondence: Peter Köhler (peter.koehler@awi.de)

References

Ahn, S., Khider, D., Lisiecki, L. E., and Lawrence, C. E.: A probabilistic Pliocene-Pleistocene stack of benthic d18O using a profile hidden Markov model, Dynamics and Statistics of the Climate System, 2, dzx002, https://doi.org/10.1093/climsys/dzx002, 2017.

Barth, A. M., Clark, P. U., Bill, N. S., He, F., and Pisias, N. G.: Climate evolution across the Mid-Brunhes Transition, Climate of the Past, 14, 2071–2087, https://doi.org/10.5194/cp-14-2071-2018, 2018.

Bintanja, R. and van de Wal, R. S. W.: North American ice-sheet dynamics and the onset of the 100,000-year glacial cycles, Nature, 454, 869–872, https://doi.org/10.1038/nature07158, 2008.

de Boer, B., Lourens, L. J., and van de Wal, R. S.: Persistent 400,000-year variability of Antarctic ice volume and the carbon cycle is revealed throughout the Plio-Pleistocene, Nature Communications, 5, 2999, https://doi.org/10.1038/ncomms3999, 2014.

EPICA-community-members: Eight glacial cycles from an Antarctic ice core, Nature, 429, 623–628, https://doi.org/10.1038/nature02599, 2004.

Flower, B. P., Oppo, D. W., McManus, J. F., Venz, K. A., Hodell, D. A., and Cullen, J. L.: North Atlantic intermediate to deep water circulation and chemical stratification during the past 1 Myr, Paleoceanography, 15, 388–403, https://doi.org/10.1029/1999PA000430, 2000.

Jouzel, J., Masson-Delmotte, V., Cattani, O., Dreyfus, G., Falourd, S., Hoffmann, G., Minster, B., Nouet, J., Barnola, J. M., Chappellaz, J., Fischer, H., Gallet, J. C., Johnsen, S., Leuenberger, M., Loulergue, L., Luethi, D., Oerter, H., Parrenin, F., Raisbeck, G., Raynaud, D., Schilt, A., Schwander, J., Selmo, E., Souchez, R., Spahni, R., Stauffer, B., Steffensen, J. P., Stenni, B., Stocker, T. F., Tison, J. L., Werner, M., and Wolff, E. W.: Orbital and millennial Antarctic climate variability over the last 800 000 years, Science, 317, 793–796, https://doi.org/10.1126/science.1141038, 2007.

Köhler, P.: Atmospheric CO_2 concentration based on boron isotopes versus simulations of the global carbon cycle during the Plio-Pleistocene, Paleoceanography and Paleoclimatology, 38, e2022PA004 439, https://doi.org/10.1029/2022PA004439, 2023.

Köhler, P. and Mulitza, S.: No detectable influence of the carbonate ion effect on changes in stable carbon isotope ratios ($\delta^{13}C$) of shallow dwelling planktic foraminifera over the past 160 kyr, Climate of the Past, 20, 991–1015, https://doi.org/10.5194/cp-20-991-2024, 2024.

Köhler, P. and Munhoven, G.: Late Pleistocene carbon cycle revisited by considering solid Earth processes, Paleoceanography and Paleoclimatology, 35, e2020PA004 020, https://doi.org/10.1029/2020PA004020, 2020.

Köhler, P., de Boer, B., von der Heydt, A. S., Stap, L. S., and van de Wal, R. S. W.: On the state dependency of equilibrium climate sensitivity during the last 5 million years, Climate of the Past, 11, 1801–1823, https://doi.org/10.5194/cp-11-1801-2015, 2015.

Lambert, F., Delmonte, B., Petit, J. R., Bigler, M., Kaufmann, P. R., Hutterli, M. A., Stocker, T. F., Ruth, U., Steffensen, J. P., and Maggi, V.: Dust-climate couplings over the past 800,000 years from the EPICA Dome C ice core, Nature, 452, 616–619, https://doi.org/10.1038/nature06763, 2008.

Lisiecki, L. E.: Atlantic overturning responses to obliquity and precession over the last 3 Myr, Paleoceanography, 29, 71–86, https://doi.org/10.1002/2013PA002505, 2014.

Lisiecki, L. E. and Raymo, M. E.: A Pliocene-Pleistocene stack of 57 globally distributed benthic $\delta^{18}O$ records, Paleoceanography, 20, PA1003, https://doi.org/10.1029/2004PA001071, 2005.

Martinez-Garcia, A., Rosell-Mele, A., Jaccard, S. L., Geibert, W., Sigman, D. M., and Haug, G. H.: Southern Ocean dust-climate coupling over the past four million years, Nature, 476, 312–315, https://doi.org/10.1038/nature10310, 2011.

McManus, J. F., Oppo, D. W., and Cullen, J. L.: A 0.5-million-year record of millennial-scale climate variability in the North Atlantic, Science, 283, 971–975, https://doi.org/10.1126/science.283.5404.971, 1999.

Mix, A. C., Le, J., and Shackleton, N. J.: Benthic foraminiferal stable isotope stratigraphy of Site 846: 0-1.8 Ma, in: Proceedings of the Ocean Drilling Program, Scientific Results Vol 138, edited by Pisias, N. G., Mayer, L., Janecek, T., Palmer-Julson, A., and van Andel, T., pp. 839–854, College Station, Texas, USA, https://doi.org/10.2973/odp.proc.sr.138.160.1995, 1995.

Poore, H. R., Samworth, R., White, N. J., Jones, S. M., and McCave, I. N.: Neogene overflow of Northern Component Water at the Greenland-Scotland Ridge, Geochem. Geophys. Geosyst., 7, Q06 010, https://doi.org/10.1029/2005GC001085, 2006.

Shackleton, N. J., Hall, M. A., and Pate, D.: Pliocene stable isotope stratigraphy of site 846, in: Proceedings of the Ocean Drilling Program, Scientific Results Vol 138, edited by Pisias, N. G., Mayer, L., Janecek, T., Palmer-Julson, A., and van Andel, T., pp. 337–355, College Station, Texas, USA, https://doi.org/10.2973/odp.proc.sr.138.1171995, 1995.

Wright, A. K. and Flower, B. P.: Surface and deep ocean circulation in the subpolar North Atlantic during the mid-Pleistocene revolution, Paleoceanography, 17, 1068, https://doi.org/10.1029/2002PA000782, 2002.

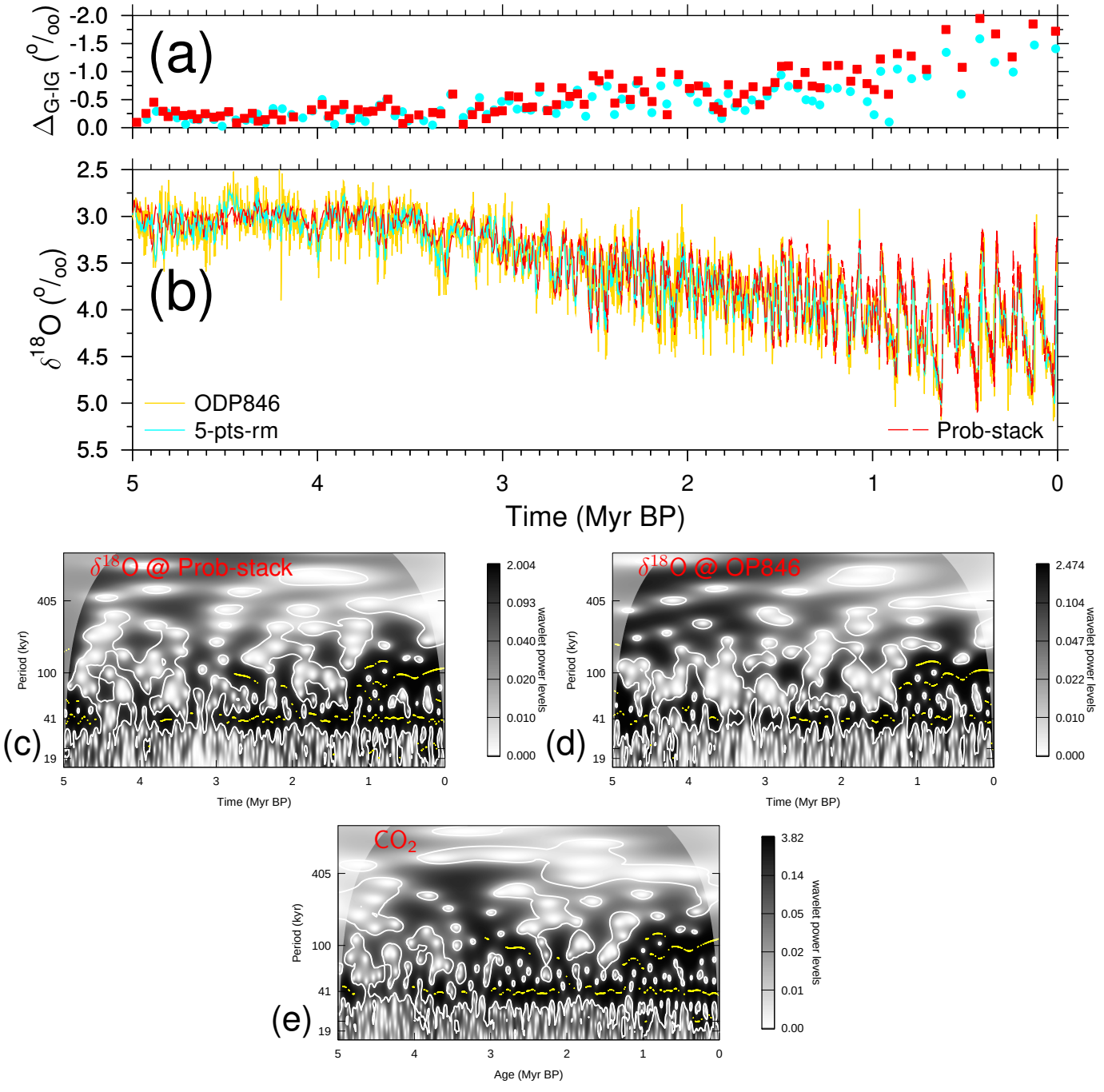

Figure S1. Climate change. (a) Glacial-interglacial amplitudes of records showing in (b). Here the difference between a glacial minima and the subsequent interglacial maxima are calculated following the MIS boundary definition of Lisiecki and Raymo (2005). Points are positions at the mid-transitions. (b) Benthic δ^{18}O from ODP846 (Mix et al., 1995; Shackleton et al., 1995; Poore et al., 2006) and Prob-stack (Ahn et al., 2017). Wavelets of detrended benthic δ^{18}O (c): Prob-stack; (d): ODP846) and (e) simulated atmospheric CO_2 (scenario SEi++V6).

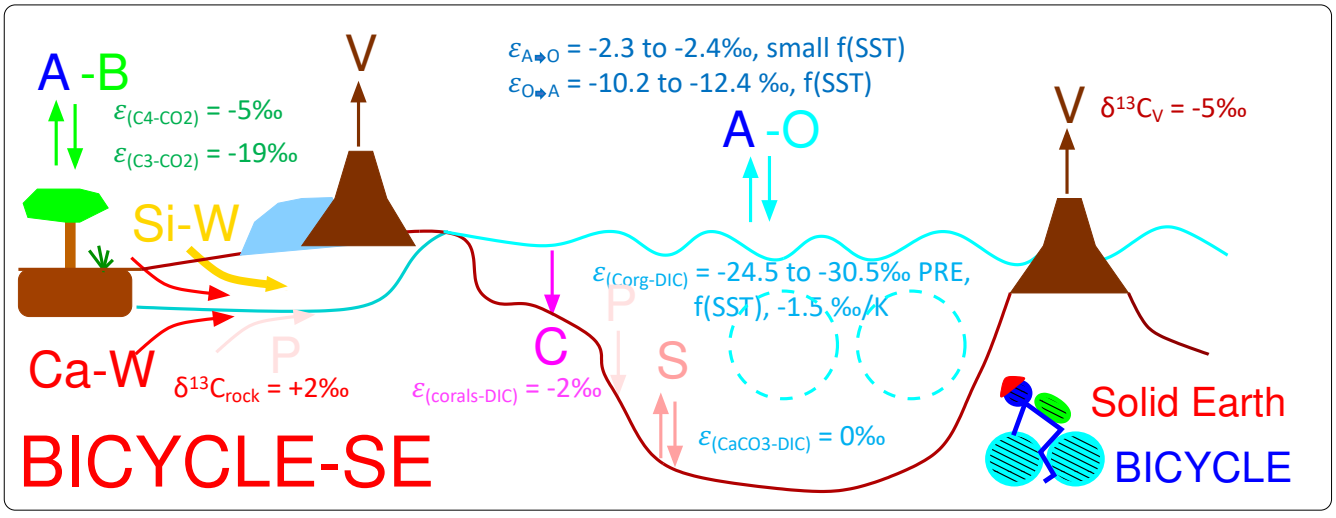

Figure S2. Sketch of the Box model of the isotopic carbon cycle, version solid Earth (BICYCLE-SE), taken from Köhler and Mulitza (2024). V: outgassing of CO_2 from volcanoes on land potentially and temporally overlain by land ice and from hot spot island volcanoes (and mid ocean ridges, not shown) influenced by changing sea level; C: shallow water carbonate deposition due to coral reef growth; Si-W: silicate weathering and Ca-W: carbonate weathering with different sources of C, but both delivering HCO_3^--ions into the ocean; P: PO_4^{3-} riverine input and sedimentary burial; S: $CaCO_3$ sedimentation and dissolution. A-B: atmosphere-biosphere exchange of CO_2; A-O: atmosphere-ocean exchange of CO_2. The cyan-coloured broken circles mimic the two overturning cell in the Atlantic and Indo-Pacific Ocean. The isotopic fractionation ε during exchange processes, or the prescribed δ^{13}C of external fluxes are given, summarising the parametrisation of the ^{13}C cycle within the model.

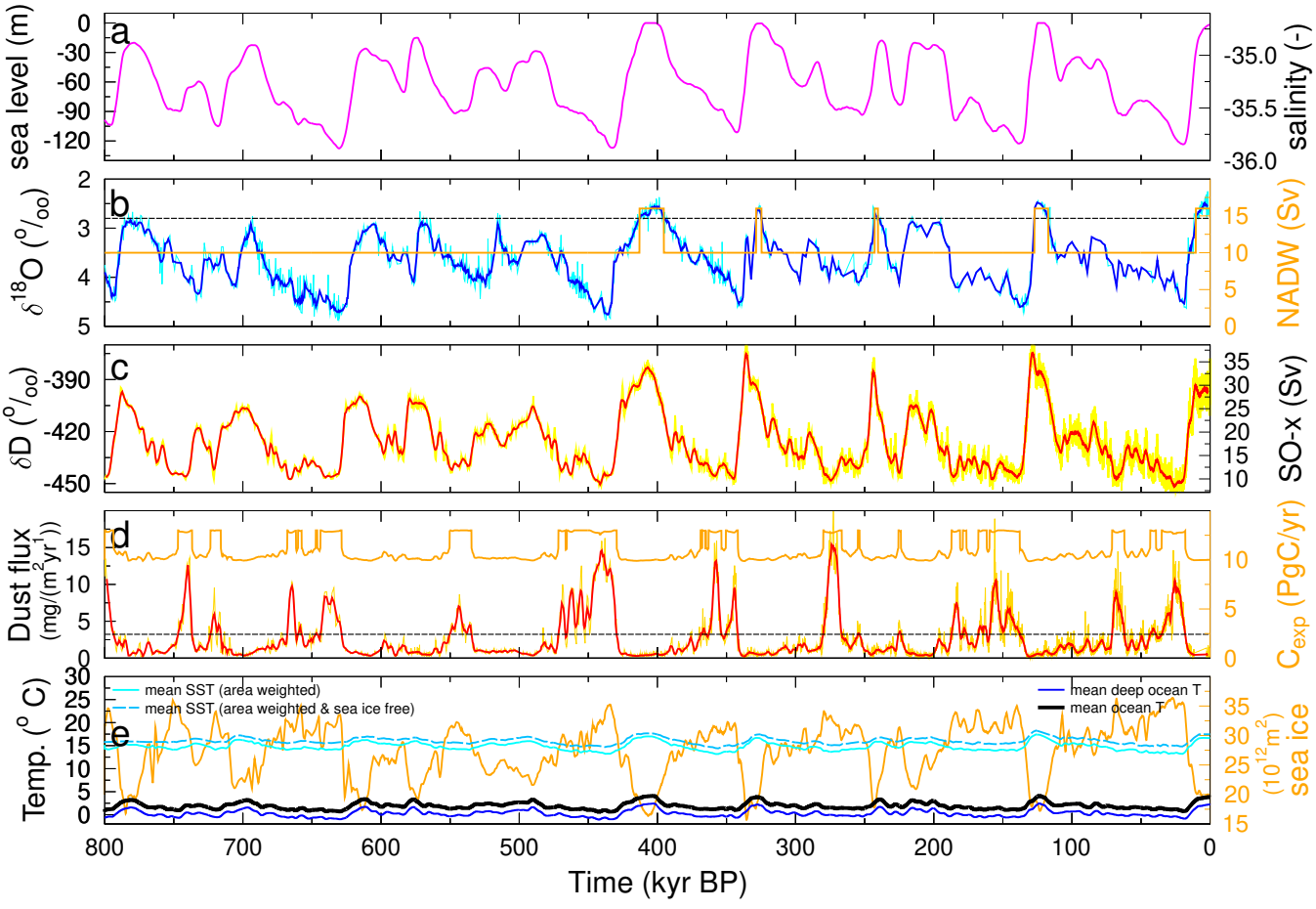

Figure S3. Time-dependent forcing of the model in scenario SEi (modified from Köhler and Munhoven (2020)). (a) Sea level following Bintanja and van de Wal (2008) resulting of corresponding mean ocean salinity (right y-axis). (b) North Atlantic Deep Water (NADW) formation is either in interglacial or glacial mode, following δ^{18}O in OPD980 (55°29′ N, 14°42′ W) (McManus et al., 1999; Flower et al., 2000; Wright and Flower, 2002), dotted line marks the threshold for switching between both states. (c) EDC ice core δD (EPICA-community-members, 2004; Jouzel et al., 2007) corrected for $\delta^{18}O_{sw}$, from which Southern Ocean sea surface temperatures (SST) and vertical mixing (SO-x: SO surface-to-deep ocean flux, right y-axis) is calculated. (d) Marine biology in the Southern Ocean (SO) is either Fe-limited or Fe-unlimited following dust fluxes in the EDC ice core (Lambert et al., 2008). The dotted line marks the threshold for switching between both states, leading to global integrated export production of organic matter at 100 m water depth (right y-axis). (e) Different ocean temperatures averaged within the model. Equatorial SST is taken from Barth et al. (2018). SST is calculated from all ocean surface boxes, deep ocean temperature from the boxes with water depths below 1000 m. The sea ice free SST is relevant for air-sea gas exchange. Right y-axis: global integrated sea ice area. In subfigures b–d original data (thin lines) and 3-kyr-running mean (bold lines) are shown. BICYCLE is forced by the running-mean data.

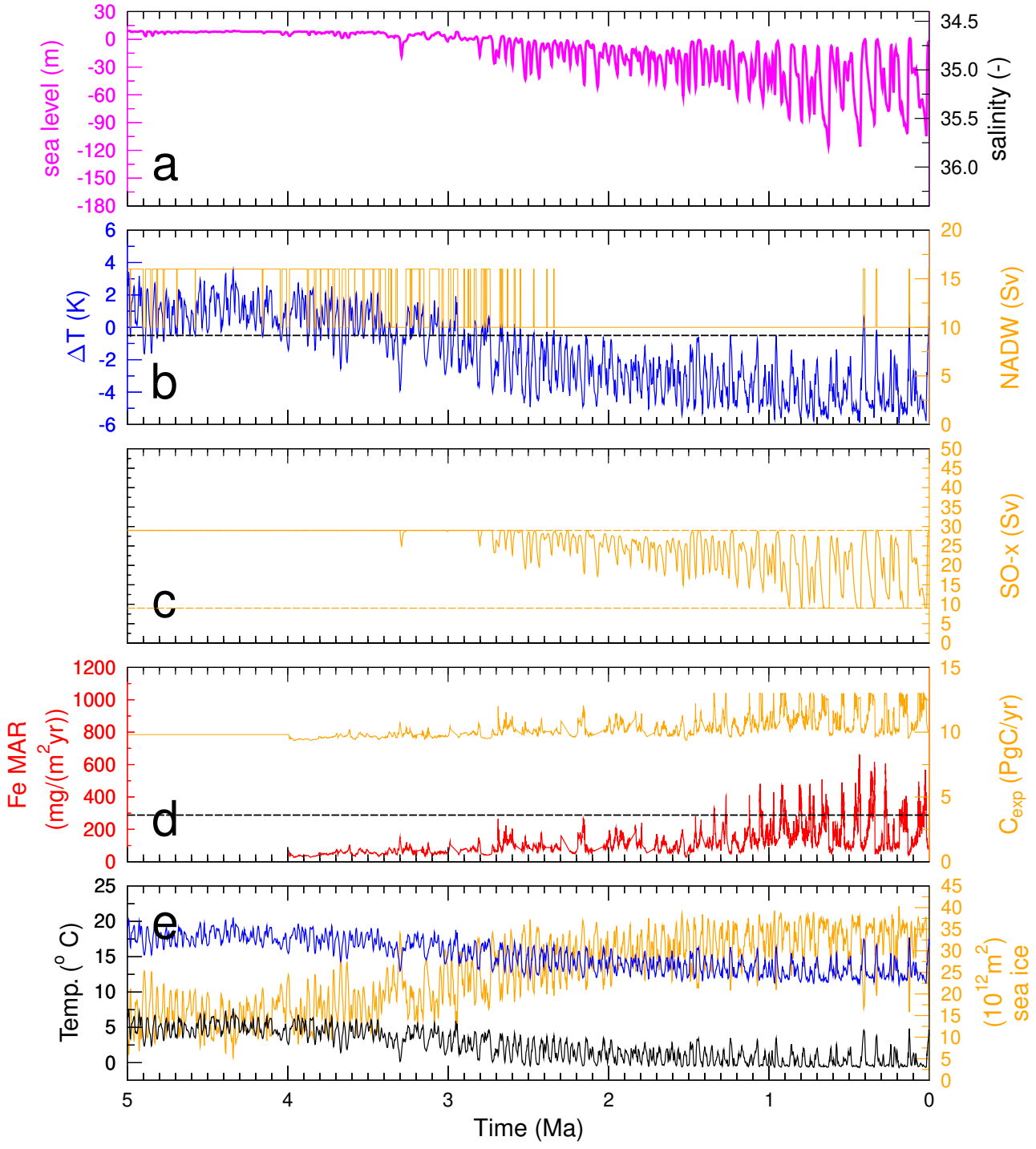

Figure S4. Time-dependent forcing of the model for scenario SEi++V6 (modified from Köhler (2023)). (a) Sea level following de Boer et al. (2014) resulting in the corresponding mean ocean salinity (right y-axis). (b) North Atlantic Deep Water (NADW) formation is either in interglacial or glacial mode, following the globally used temperature record (blue) from Köhler et al. (2015), broken line marks the threshold for switching between both states. (c) Southern Ocean vertical mixing (SO-x: SO surface-to-deep ocean flux, right y-axis) is calculated with upper and lower limitation (9–29 Sv), marked by horizontal lines. Here, the vertical mixing is calculated as function of sea level. (d) Marine biology in the Southern Ocean (SO) is either Fe-limited or Fe-unlimited following Fe MAR in ODP1090 (Martinez-Garcia et al., 2011). The dotted line marks the threshold for switching between both states, leading to global integrated export production of organic matter at 100 m water depth (right y-axis). (e) Ocean temperatures averaged within the model (mean ocean (black), area weighted mean SST (blue)). Right y-axis: global integrated sea ice area.

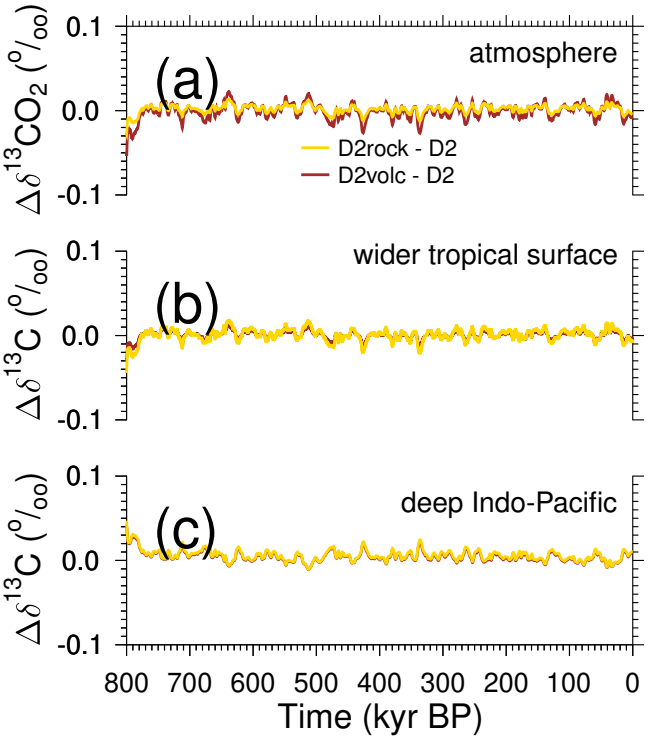

Figure S5. Consistency check. Differences in simulated (a) atmospheric $\delta^{13}CO_2$, (b) wider tropical surface ocean $\delta^{13}C$ and (c) deep Indo-Pacific $\delta^{13}C$ when forcing the model with in post-processing calculated $\delta^{13}C_{rock}$ (D2rock) or the $\delta^{13}C_v$ (D2volc) with respect to D2, the scenarios in which the isotopic signatures have been generated.

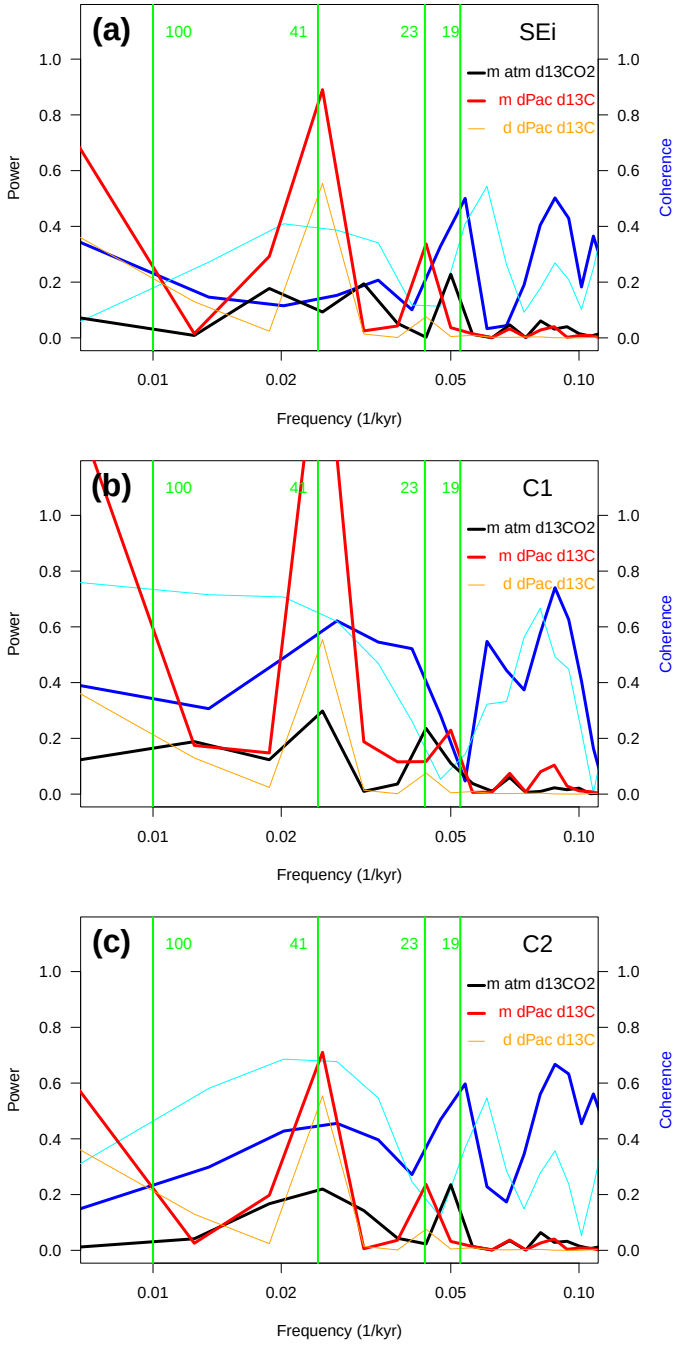

Figure S6. Spectral and coherence analysis for the last 150 kyr of scenarios (a) SEi, (b) C1, (c) C2. Atmospheric $\delta^{13}CO_2$ in the model (m) against deep Indo-Pacific $\delta^{13}C$ in the model or in the data (d), where data is the 6 cores stack from Lisiecki (2014).